Deep learning-based intelligent evaluation of freeze-thaw damage in tunnel lining using PZT-induced stress wave

Xiaolong Liao[1]
Key Laboratory of Transportation Tunnel Engineering, Ministry of Education, Southwest Jiaotong University, Chengdu 610031, China; email: liaoxiaolong@my.swjtu.edu.cn

Haojia Zhong[2]
Department of Civil Engineering, The University of Hong Kong, Pokfulam 999077, China; e-mail: hku.haojia@gmail.com

Yifeng Zhang[3]
Zachry Department of Civil & Environmental Engineering, Texas A&M University, College Station, TX 77843; e-mail: tamu.zyf@gmail.com

Chuan Zhang[4,*](corresponding author)
Key Laboratory of Transportation Tunnel Engineering, Ministry of Education, Southwest Jiaotong University, Chengdu 610031, China; e-mail: zhangchuan@my.swjtu.edu.cn

Qixiang Yan[5]
Key Laboratory of Transportation Tunnel Engineering, Ministry of Education, Southwest Jiaotong University, Chengdu 610031, China; e-mail: yanqixiang@home.swjtu.edu.cn

ABSTRACT

Tunnel lining structures in cold regions are frequently damaged by freeze-thaw (f-t) cycles, which have emerged as one of the main factors to affect the service life of tunnels. Real-time and accurate evaluation of such damage is of great importance for the development of effective maintenance strategies. In this paper, we proposed a novel deep learning-based intelligent method to evaluate the f-t damage in tunnel lining using PZT-induced stress wave. First of all, f-t cycle durability experiments were conducted on the tunnel lining concrete, during which the stress wave signals were measured using PZT transducers. The waveform and energy change rule of the stress wave signals during the f-t cycle were analyzed. After that, the time-frequency diagrams were generated from the collected signals through the continuous wavelet transform (CWT). Meanwhile, a fine-scale numerical model was proposed to simulate concrete f-t damage process, and the damage stages were divided based on the simulated damage unit area. As a result, a CWT-based image dataset with damage stage labels was established. In addition, a convolutional neural network (CNN) model was developed for automatically extracting features from the CWT images and ultimately predicting the f-t damage stage. Finally, the performance of the CNN model was compared with two machine learning algorithms including support vector machine (SVM) and back-propagation neural network (BPNN). The results show that the CNN model can accurately predict the concrete f-t damage stage and has superior performances over other methods, indicating its great potential for real-time monitoring and rapid evaluation of concrete f-t damage in tunnel lining.

KEYWORDS: Deep learning; F-t damage; Automatic evaluation; PZT transducer; Concrete structures

1. INTRODUCTION

In cold climates, tunnel lining structures are susceptible to damage by freeze-thaw (f-t) cycling, which has become one of the main factors that reduce the durability of tunnel lining (Wang, Hu, Li, Wang and Zhang, 2022). F-t damage not only reduces the mechanical properties of lining

concrete, but also increases its permeability and corrosion risk, thus posing a potential threat to the safety and stability of tunnel lining structures (Liu, Tu, Sas and Elfgren, 2021). Therefore, accurate and timely evaluation of f-t damage to tunnel lining structures in cold regions is critical because it can reveal potential hazards and enable engineers to make timely repair decisions.

Recent years have witnessed the rapid development of a transducer called Lead Zirconate Titanate (PZT), which is capable of real-time, continuous monitoring for a variety of structures (Song, Mo, Otero and Gu, 2006, Li, Wang, Liu and Luo, 2020). PZT-based transducers can be easily mounted on surfaces or embedded in structures and offer the advantages of cost-effectiveness, broad band coverage and fast response times (Li, Fan, Ho, Wu and Song, 2017, Zhang, Panda, Yan, Zhang, Vipulanandan and Song, 2020). One common monitoring technique that utilizes PZT transducers is called the wave propagation technique, also known as active sensing method. This method is featured by a high degree of sensitivity to variations in structural and material properties. Numerous successful applications in concrete crack development monitoring (Zhang, Li, Kang and Zhang, 2022, Zhang, Wang, Li and Kang, 2023), joint mechanical behavior monitoring (Gao, Zhang and Chen, 2023), concrete corrosion damage measurements (Jiang, Kong, Peng, Wang, Dai, Feng, Huo and Song, 2017, Zou, Cheng, Liu, Qin and Yi, 2019), structural health assessment under seismic excitation (Liao, Wang, Song, Gu, Olmi, Mo, Chang and Loh, 2011), cementitious materials curing process and strength gain monitoring (Kong, Hou, Ji, Mo and Song, 2013, Wang, Jiang, Cui, Yang and Yang, 2022, Liao, Yan, Zhong, Zhang and Zhang, 2023) have confirmed the solid advantages of this approach. However, there are very few studies on the application of this approach to monitor concrete f-t damage. In addition, current research based on active sensing approach relies on manually extracting useful information from stress wave signals. The hand-crafted features, while reflecting the state of the structure to some extent, are prone to lose some key information and give a misclassification of the structural state. Therefore, it is of great significance to develop an intelligent technique that can automatically extract sensitive features from a large amount of monitoring data and accurately identify structural damage.

Deep learning (DL) technique offers the potential for the processing of large amounts of monitoring data generated in structural health monitoring (SHM) (Zhou, Huang, Wang and Xia, 2022, Nguyen, Ta, Ho, Kim and Huynh, 2023, Liao, Yan, Zhang, Zhong, Qi and Wang, 2023). Many scholars have contributed meaningful work on SHM by utilizing DL techniques. For example, Zhang et al. (Zhang, Miyamori, Mikami and Saito, 2019) introduced a one-dimensional convolutional neural network (1D-CNN) approach to identify structural damage using vibration data. Ai et al. (Ai, Mo, Han and Wen, 2022) devised a 2D-CNN model, combining it with electromechanical admittance data (EMA), to detect compressive stresses and load-induced damage in concrete structures. Nguyen et al. (Nguyen, Tuong Vy Phan, Ho, Man Singh Pradhan and Huynh, 2022) proposed a DL-based method for automated sensitive feature extraction to monitor prestress in reinforced concrete (RC) girders using raw impedance signals. Ai et al. (Ai, Soltangharaei and Ziehl, 2022) introduced an ensemble learning model that integrates CNN and random forest to assess concrete damage caused by Alkali-silica reaction using acoustic emission data. Chen et al. (Chen, Shen, Huo and Narazaki, 2023) developed a DL-based detector, incorporating dilated convolution (DC) and class activation map (CAM), to identify voids in concrete columnar structures through percussion-induced sound signals. The aforementioned literature illustrates the feasibility and promising applications of DL algorithms for identifying structural health states. However, few studies have explored the integration of DL techniques with active sensing approaches for structural damage monitoring, let alone the evaluation of f-t (f-t) damage in concrete materials.

The aim of this study is to investigate an intelligent method for the evaluation of f-t damage in tunnel lining concrete. For this purpose, the PZT-based wave propagation technique and DL technique are combined. Specifically, f-t cycle durability experiments were conducted on tunnel lining concrete and stress wave signals were measured during the f-t cycle process using PZT transducers. The stress wave signal variation during f-t cycling was analyzed. The collected signals were then converted into time-frequency maps using continuous wavelet transform (CWT) and the f-t damage was divided into four stages using a fine-scale numerical model.

Subsequently, the corresponding CWT image samples were divided at each stage, thus creating a CWT image-based dataset. In addition, a CNN model was built to automatically extract features from the CWT images and finally predict the f-t damage stage. Finally, the performance of the CNN model is evaluated and compared with two machine-based methods.

2. PZT-BASED WAVE PROPAGATION TECHNIQUE

In this paper, we employ the PZT-based wave propagation technique to monitor f-t damage in tunnel lining concrete. This approach requires a minimum of two PZT transducers, which can be either affixed to the concrete surface or embedded within it. One of these transducers functions as an actuator, receiving a transient AC voltage from an external source via a wire. When exposed to alternating electrical signals, the actuator generates harmonic vibrations through the inverse piezoelectric effect, thereby generating solid stress waves within the concrete medium. On the opposing side of the concrete structure, another PZT transducer is positioned. This secondary transducer can convert the received stress wave into a time-domain voltage signal using the positive piezoelectric effect. During f-t cycles, the pore and capillary water inside the concrete undergo repeated freezing and thawing, leading to fluctuating internal expansion stresses. If these expansion stresses exceed the tensile strength of the pore structure, it can result in irreversible microcracks or even large cracks in the concrete. As the stress wave propagates through the concrete, these cracks and pore irregularities reflect, transmit, and diffract the stress wave, ultimately causing changes in the waveform of the received stress signal. By analyzing the signal characteristics following different f-t cycles, it is possible to assess the concrete's damage state.

3. THE PROPOSED DL-BASED F-T DAMAGE EVALUATION METHOD

Figure 1 demonstrates the flow of the proposed DL-based f-t damage evaluation method in this paper. Firstly, the stress wave signals were continuously measured during f-t cycles using the PZT-based wave propagation technique. Subsequently, the acquired stress wave signals were transformed into 2D time-frequency spectra by CWT. Meanwhile, a fine-scale numerical model was adopted to simulate concrete f-t damage process, and the f-t damage were divided into four stages based on the simulated damage unit area. The processed signals were then assigned corresponding damage stage labels to form complete data pairs. After that, a CNN model was constructed to perform feature extraction on the time-frequency spectrum and ultimately classify the f-t damage stages.

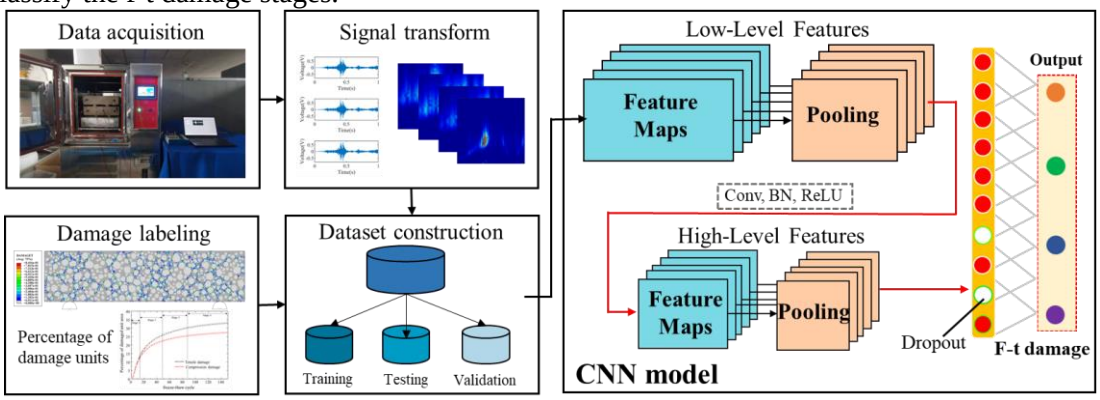

Figure 1 The proposed DL-based f-t damage evaluation method

3.1 *Continuous wavelet transform*

CWT is utilized to transform the stress wave signals into 2D time-frequency images to satisfy

the input form of the CNN model. Compared to the original time-domain signal, the time-frequency spectrum obtained from CWT provides more comprehensive information both in time-frequency domain. The CWT of a 1D time-series signal x(t) can be defined by the following Eq. (1):

$$CWT(a,\tau)=\frac{1}{\sqrt{a}}\int_{-\infty}^{\infty}x(t)\psi(\frac{t-\tau}{a})d_t=\left\langle x(t),\psi_{a,\tau}(t)\right\rangle \tag{1}$$

where $\psi_{a,\tau}(t)$ is the wavelet basis, a denote the scale index controlling wavelet function scaling, and τ refers to the translation parameter for controlling time-shifting.

3.2 Convolutional neural network

CNN is one of the most representative of DL methods, which is essentially a supervised model of feed-forward neural network with an interlayer feature information transfer mechanism inspired by animal visual cortex. It is widely utilized due to its great advantages in image processing. Figure 2 illustrates the detailed structure of the CNN, which contains five main parts: input layer, convolutional layer, pooling layer, fully connected (FC) layer and output layer. The convolutional layer is used for feature extraction, and the pooling layer is responsible for reducing the data dimensionality, which can be used interchangeably to improve feature extraction and efficiency performance. In addition, the convolutional and FC layers are usually followed by a normalized batch (BN) layer and a dropout layer, respectively, which helps to improve efficiency and avoid overfitting.

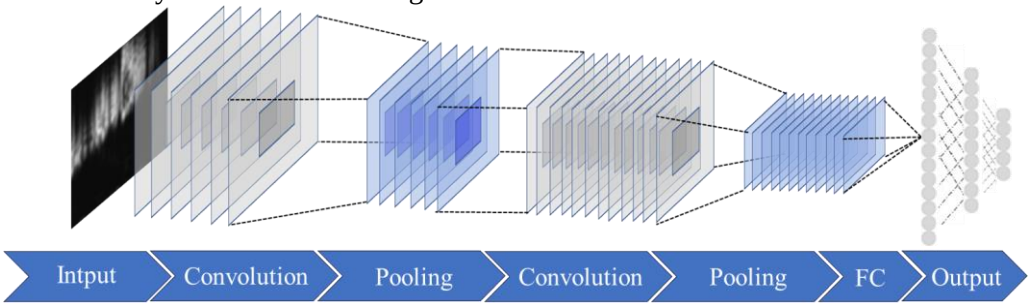

Figure 2 CNN architecture

The convolution operation is a key procedure in CNN. In the convolutional layer, a feature matrix containing one or more sets of features can be given as input, and the output feature matrix of the layer is generated by convolving multiple sets of learnable convolutional kernels and forming a 2D tensor. The convolutional layer contains two important characteristics: weight sharing and local connectivity, which ensure its high computational efficiency and robustness. The mathematical formulas Eq. (2) and Eq. (3) for the convolution calculation are as follows:

$$x_k^l=\sum_{i=1}^{N}conv2D(w_{ik}^{l-1},s_i^{l-1})+b_k^l \tag{2}$$

$$y_k^l=f(x_k^l) \tag{3}$$

where x_k^l is the output before activation, w_{ik}^{l-1} represents the filters, s_i^{l-1} denotes the output of previous layer, b_k^l is the bias, $conv2D(,)$ refers to 2D convolution, y_k^l denotes the output after activation, $f(\cdot)$ is defined as activation function.

After implementing feature extraction, a large number of high-dimensional feature maps will be formed. To reduce the computational effort, these feature maps will be down-sampled at the pooling layer. The operation of the pooling layer can drastically reduce the training parameters while keeping the feature map space invariant, thus preventing overfitting to a large extent. The down-sampled can be expressed as Eq. (4):

$$s_k^l = y_k^l \downarrow ss \tag{4}$$

where s_k^l represents the output after pooling, $\downarrow ss$ denotes the down-sampled operation.

The last layers of CNN are usually connected by a fully connected layer that classifies the features. Behind the pooling layer, the output feature matrix is flattened into a vector that serves as the input to the fully connected layer. Finally, the softmax function is used to transform the output values of multiple categories to a probability distribution in the range [0, 1]. It can be defined with the following Eq. (5):

$$o_i^{(l+1)} = softmax(z_i^{(l+1)}) = \frac{\exp(z_i^{(l+1)})}{\sum_{c=1}^{C} \exp(z_i^{(l+1)})} \tag{5}$$

where o_i is the final output, C represents the number of output nodes, i.e., classification categories.

4. EXPERIMENTAL SCHEME

The prismatic specimens with dimensions of 400 × 100 × 100 mm^3 were prepared for the experiments in this paper. The raw materials used in the specimens include cement, fine and coarse aggregates, water reducing agent and water. The corresponding mixing proportions are 1:1.70:0.94:0.38. The cement used in the experiment is ordinary Portland cement provided by Lafarge, with a strength grade of 42.5. The fine aggregate is a mixture of fine sand and medium sand. The ratio of fine sand to medium sand in the mixture is 3:2. The coarse aggregate is made up of continuously graded aggregates ranging in size from 5mm to 20mm. The above ingredients were mixed evenly in an electric blender with pure water and the high-performance polycarboxylate plasticizer was added during the process to improve compatibility.

Two circular PZT patches, each with a radius of 10.0 mm and a thickness of 1.0 mm, were embedded at the appropriate locations at each end of the specimen. Prior to installing these PZT transducers into the concrete specimen, each transducer was electrically insulated by applying a layer of liquid electrical tape to its surface. Figure 3 depicts the specific position about the PZT transducer in the specimen. In the figure, the two PZT patches are arranged with their circular surfaces opposing each other and aligned in a straight line. One patch serves as the actuator (PZT 1), while the other serves as the sensor (PZT 2). After installing all the devices, the freshly mixed concrete was cast in the molds and left to shape for 24 hours. Thereafter, the specimens were demolded and experienced a curing process for 28 days in a standard curing condition.

The concrete specimens underwent f-t cycle testing in a programmable constant temperature and humidity chamber. The f-t procedure entailed subjecting the specimens to 150 cycles of rapid freezing and thawing, with each cycle lasting 4 hours and the f-t temperature ranging between -20 °C and 20 °C. The stress wave signal measurement equipment included a data acquisition board (NI USB-6366), two PZT transducers and a laptop. Figure 2 shows the experimental scheme for stress wave signal acquisition. During the measurement, one of the embedded sensors (PZT1) operates as an exciter to generate a sinusoidal sweep, while the other (PZT2) acts as a transducer to receive the response signal. The computer-controlled NI USB-6366 board was responsible for generating the sweeping sine wave, with a frequency range of 100 Hz-250 kHz, amplitude of 10 V and sweep period of 1 s. The data acquisition system sampled the signals at a frequency of 1 MHz. At the completion of the f-t cycles, a total of 150 sets of stress wave signals were collected.

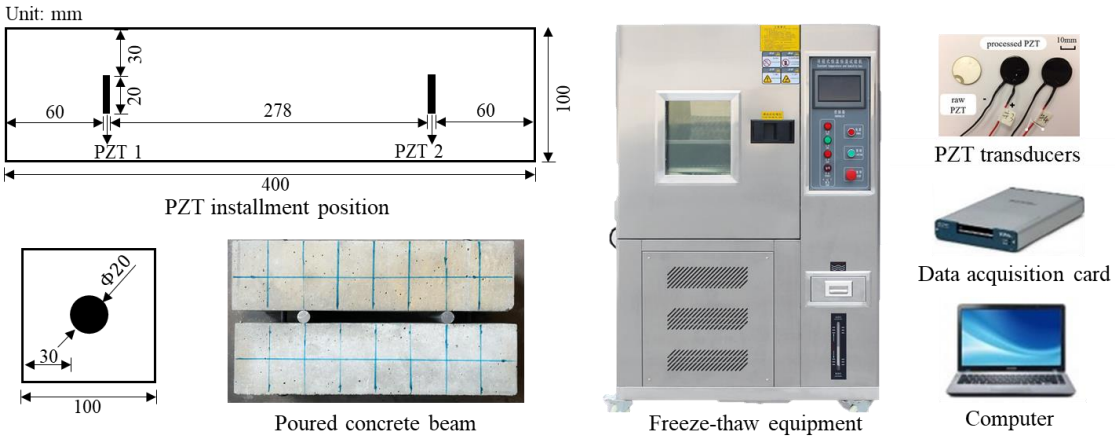

Figure 3 Experimental materials and equipment

5. RESULTS AND ANALYSIS

5.1 *Stress wave variation*

The time-domain waveforms and signal energy variation of the received stress wave during the f-t cycles process are shown in Figure 4. The time-domain waveform shows that the maximum amplitude of the signal remains relatively stable during the first 50 f-t cycle. After this point, a significant decrease in the maximum amplitude can be observed, indicating that the formation of frost cracks affects the propagation of the stress wave. After the 150 f-t cycle, the maximum amplitude of the signal reaches a minimum. In addition, the signal energy change shows that there is a slight increase in signal energy during the first 50 cycles. This may be due to the fact that the cold environment causes the concrete to shrink and become dense before the formation of frost cracks. After that, the signal energy decreases monotonically until 150 f-t cycles. This indicates that the f-t environment has caused damage and cracks in the concrete, absorbing the energy to propagate the signal.

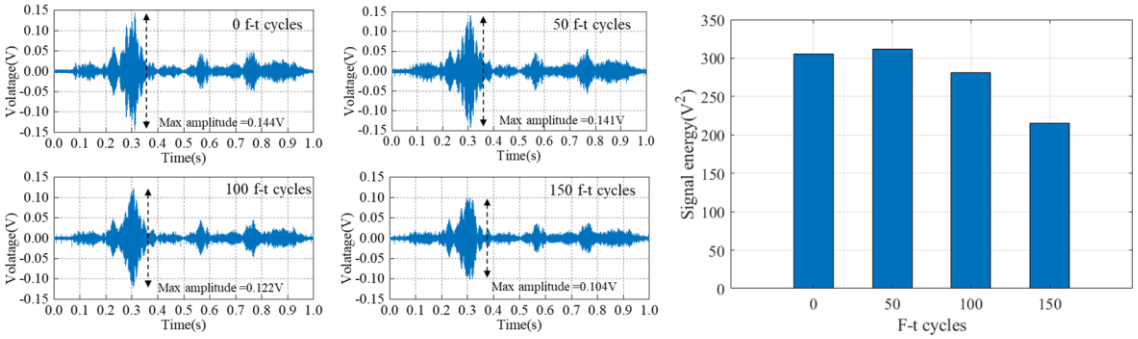

Figure 4 Stress wave and signal energy variation during the f-t cycles process

5.2 *Numerical model-based damage labeling*

The finite element method is adopted to simulate the f-t damage process of concrete. To develop concrete fine-scale model, the concrete is considered to be composed of the following three components: concrete mortar, aggregates and interfacial transition zone (ITZ). To simplify the calculations, all the components were considered in two dimensions. A mesh-based approach for modeling concrete coarse aggregates was used to generate aggregate concave and convex shapes. Polygonal aggregates are then randomly placed into the mortar area. Figure 5 illustrates a schematic of the fine-scale numerical model of concrete.

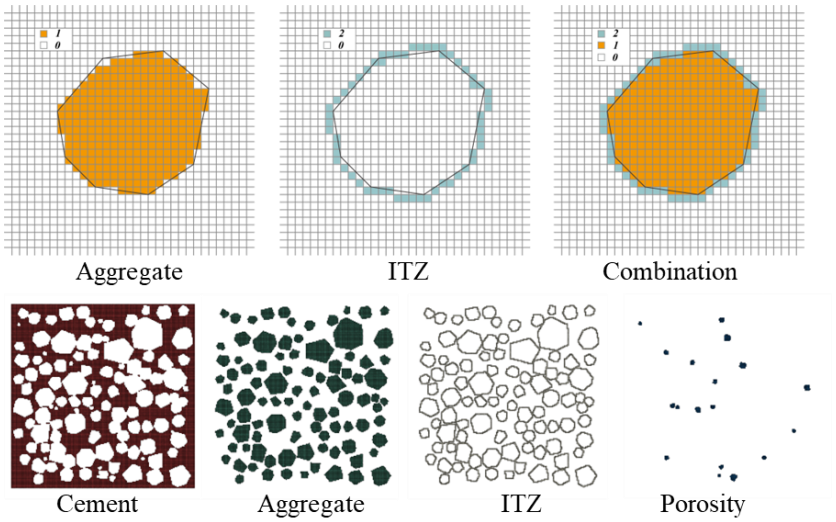

Figure 5 Fine-scale numerical model of concrete

It is difficult to directly realize the process of ice-water phase transition of pore water and continuous pore expansion during f-t cycles in numerical simulations. In this paper, the following assumptions are made: (1) It is assumed that the water expansion coefficient in the pores remains fixed during each f-t cycle; (2) Water is assumed to remain as fully filled in the pores throughout the temperature change. In order to more realistically realize the expansion and contraction of pore water during f-t cycles, it can be assumed that the pore unit is the ice-water unit, and the ice-water unit appears to melt and freeze repeatedly with the change of ambient temperature. In addition, to simulate the continuous volume expansion of the ice-water unit during repeated freezing and melting, the expansion coefficients of melting and freezing need to be set differently. Based on the subroutine UEXPAN program control of ABAQUS, we implemented the phase transition simulation of the pore unit as shown in Figure 6.

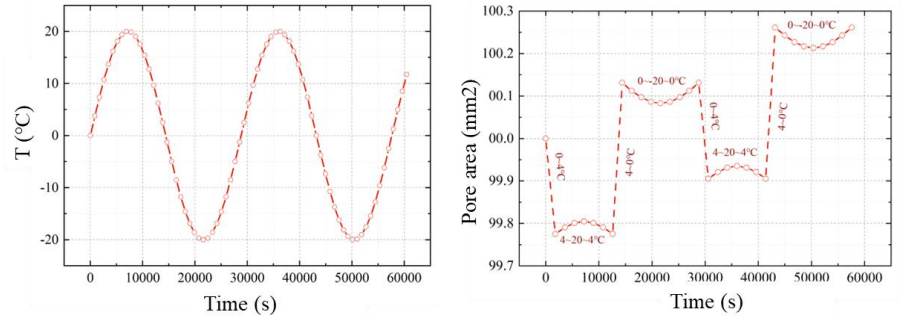

Figure 6 Temperature and pore area changes during f-t cycles

The simulation of f-t damage was performed based on concrete damaged plasticity (CDP) model in ABAQUS software and the stiffness degradation was used to reflect the strength degradation of the material. The dimensions and parameters of the model are consistent with the experimental design in Section 4. Figure 7 shows the results of f-t damage simulation of concrete beams. The results demonstrated the trend of compression damage and tensile damage with the increase of the number of f-t cycles. To verify the validity of the fine-scale numerical model in this paper, the simulated flexural strengths were compared with the results obtained from experiments, as shown in Figure 8. It can be seen that the simulated and experimental results are essentially consistent, which verifies the validity of the fine-scale f-t damage numerical model. Further, we extracted the proportion of the total cell area accounted for the damaged cell area and divided the f-t damage process into four stages as shown in Figure 9.

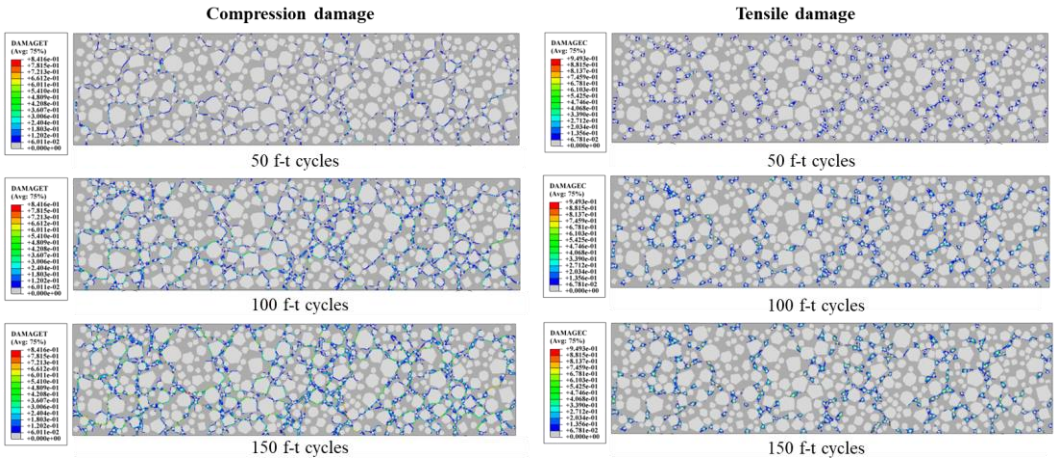

Figure 7 Simulation results of f-t damage of concrete beams

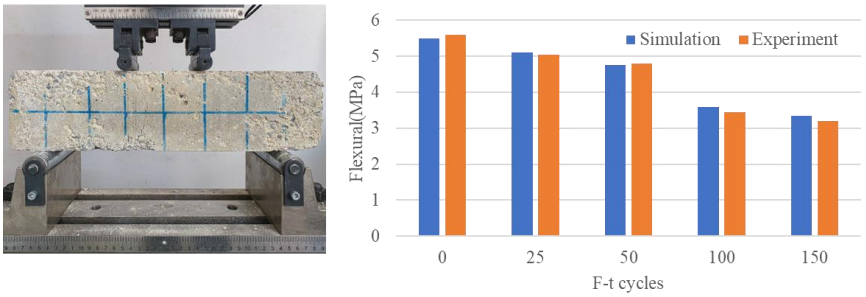

Figure 8 Flexural experiment and corresponding simulations and experimental results

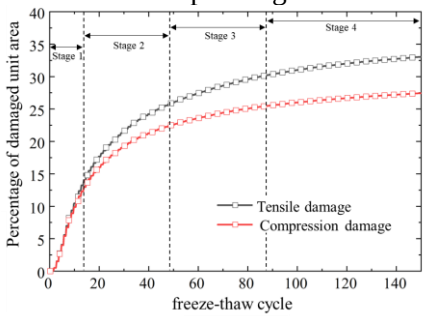

Figure 9 Damage unit area change amount and stage division

5.3 *DL-based f-t damage evaluation results*

The implementation of the proposed DL-based f-t damage evaluation method mainly includes the following steps: dataset construction, model training, and damage evaluation. In the dataset construction stage, we carried out data enhancement to the raw data through noise addition. For this purpose, a total of 600 data were obtained. These data were then transformed by CWT to form time-frequency images. These time-frequency images corresponded one-to-one with the labels obtained based on the numerical damaged model. Subsequently, the dataset was divided into training set and test set in the ratio of 3:2. The training set was used for CNN training and the test set was used to evaluate the performance. In addition, two machine learning algorithms, i.e., support vector machine (SVM) and back-propagation neural network (BPNN), were adopted for comparison. Figure 10 shows the confusion matrix of the prediction results of these three methods. It can be seen that the CNN model has higher classification accuracy compared to SVM and BPNN. In addition, it can also be seen from Table 1 that the CNN model can achieve a classification accuracy of 94.1%, which is significantly better than the remaining two algorithms.

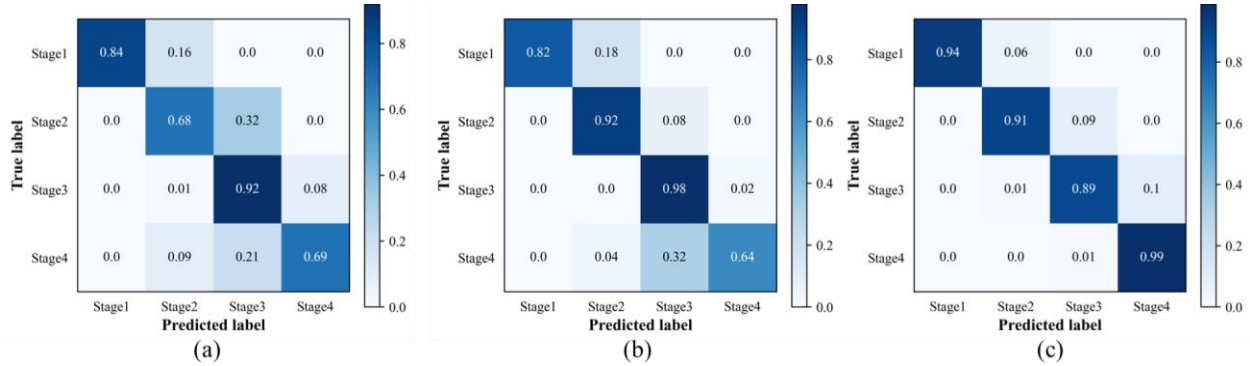

(a) (b) (c)

Figure 10 Confusion matrix of prediction results: (a) SVM, (b) BPNN, (c) CNN

Table 1 Evaluation performances of different methods

Methods	SVM (%)	BPNN (%)	CNN (%)
Accuracy	78.4	83.9	94.1
Precision	81.1	87.2	94.5
Recall	78.3	83.9	94.1
F1-score	78.5	83.8	94.3

Figure 11 shows the visualized maps of learned features in CNN. It can be observed from this figure that the feature maps in the first conventional layer heavily preserves the characteristics of the raw input CWT image. In comparison, the features extracted by the second convolutional layer are more abstract. These variations in the feature maps indicate that the mechanism of CNN is the process of extracting shallow features from CWT images to deeper features. Shallow features usually include basic information such as shape, color, etc., and are not yet capable of characterizing damage process, while deep features contain more distinguishable information, which helps to identify concrete f-t damage.

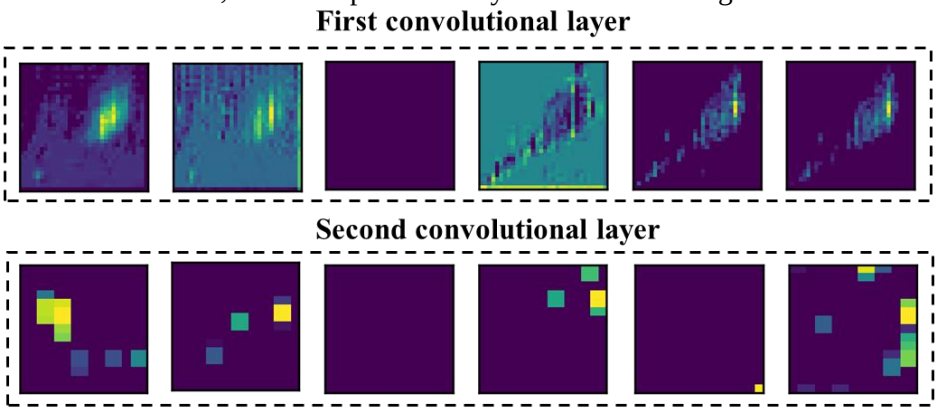

Figure 11 Visualization of feature maps

6. CONCLUSION AND FUTURE WORKS

This paper investigates the applicability and effectiveness of integrating PZT-based wave propagation with DL techniques for evaluating f-t damage in tunnel lining concrete. F-t cycle durability tests were conducted on the tunnel lining concrete and stress wave signals were measured during the f-t cycle process using PZT transducers. The waveform and energy change rule of the received stress wave signals were analyzed. The results show that the signal waveform changes significantly as the f-t cycle proceeds, along with a decrease in signal energy. The acquired signals were then processed by data enhancement and the processed signals were converted into time-frequency maps using CWT. Further, these CWT image samples were categorized into four types corresponding to the four stages of concrete f-t damage based on a fine-scale numerical model. More importantly, a CNN model was developed for automatically extracting features from the CWT images and ultimately predicting the f-t damage stage of

concrete. Finally, the performance of the CNN model was compared with SVM and BPNN. The results show that the CNN model can accurately predict the concrete f-t damage stage and has better prediction accuracy compared to the remaining two machine learning algorithms.

Future work will focus on the following areas: (1) collecting a wider range of data sets, including different concrete mixtures and varying environmental conditions to facilitate the applicability of the proposed method to different types of tunnel linings; (2) considering the incorporation of migration learning methods, as they can improve the generalization of the model, especially when dealing with sparse or expensive data. (3) optimizing the model configuration to reduce computational effort while maintaining high accuracy.

CONFLICT OF INTERESTS

The authors declare no conflict of interests.

ACKNOWLEDGEMENTS

This research is supported by the National Natural Science Foundation of China (Grant Number: U21A20152, 52278416, 52208407) and the China Postdoctoral Science Foundation (2022 M712640).

REFERENCES

Ai, D., Mo, F., Han, Y., Wen, J., and Junjie, W. 2022. Automated identification of compressive stress and damage in concrete specimen using convolutional neural network learned electromechanical admittance. *Engineering Structures*, 259: 113173.

Ai, L., Soltangharaei, V., and Ziehl, P. 2022. Developing a heterogeneous ensemble learning framework to evaluate alkali-silica reaction damage in concrete using acoustic emission signals. *Mechanical Systems and Signal Processing*, 172: 108981.

Chen, D., Shen, Z., Huo, L., and Narazaki, Y. 2023. Percussion-based quasi real-time void detection for concrete-filled steel tubular structures using dense learned features. *Engineering Structures*, 274, 115197.

Gao, W., Zhang, C., and Chen, L. 2023. Monitoring mechanical behaviors of CLT connections under reciprocating loading based on PZT-enabled active sensing and machine learning algorithms. *Smart Materials and Structures*, 32(2), 024001.

Jiang, T., Kong, Q., Peng, Z., Wang, L., Dai, L., Feng, Q., Huo, L., and Song, G. 2017. Monitoring of Corrosion-Induced Degradation in Prestressed Concrete Structure Using Embedded Piezoceramic-Based Transducers. *IEEE Sensors Journal*, 17(18), 5823-5830.

Kong, Q., Hou, S., Ji, Q., Mo, Y. L., and Song, G. 2013. Very early age concrete hydration characterization monitoring using piezoceramic based smart aggregates. *Smart Materials and Structures*, 22(8), 085025.

Li, W., Fan, S., Ho, S. C. M., Wu, J., and Song, G. 2017. Interfacial debonding detection in fiber-reinforced polymer rebar–reinforced concrete using electro-mechanical impedance technique. *Structural Health Monitoring*, 17(3), 461-471.

Li, W., Wang, J., Liu, T., and Luo, M. 2020. Electromechanical impedance instrumented circular piezoelectric-metal transducer for corrosion monitoring: modeling and validation. *Smart Materials and Structures*, 29(3), 035008.

Liao, W.-I., Wang, J. X., Song, G., Gu, H., Olmi, C., Mo, Y. L., Chang, K. C., and Loh, C. H. 2011. Structural health monitoring of concrete columns subjected to seismic excitations using piezoceramic-based sensors. *Smart Materials and Structures*, 20(12), 125015.

Liao, X., Yan, Q., Zhang, Y., Zhong, H., Qi, M., and Wang, C. 2023. An innovative deep neural network coordinating with percussion-based technique for automatic detection of concrete

cavity defects. *Construction and Building Materials*, 400, 132700.
Liao, X., Yan, Q., Zhong, H., Zhang, Y., and Zhang, C. 2023. Integrating PZT-enabled active sensing with deep learning techniques for automatic monitoring and assessment of early-age concrete strength. *Measurement*, 211, 112657.
Liu, D., Tu, Y., Sas, G., and Elfgren, L. 2021. Freeze-thaw damage evaluation and model creation for concrete exposed to freeze–thaw cycles at early-age. *Construction and Building Materials*, 312, 125352.
Nguyen, T.-T., Tuong Vy Phan, T., Ho, D.-D., Man Singh Pradhan, A., and Huynh, T.-C. 2022. Deep learning-based autonomous damage-sensitive feature extraction for impedance-based prestress monitoring. *Engineering Structures*, 259, 114172.
Song, G., Mo, Y. L., Otero, K., and Gu, H. 2006. Health monitoring and rehabilitation of a concrete structure using intelligent materials. Smart Materials and Structures, 15(2), 309-314.
Wang, J., Jiang, S., Cui, E., Yang, W., and Yang, Z. 2022. Strength gain monitoring and construction quality evaluation on non-dispersible underwater concrete using PZT sensors. *Construction and Building Materials*, 322, 126400.
Wang, R., Hu, Z., Li, Y., Wang, K., and Zhang, H. 2022. Review on the deterioration and approaches to enhance the durability of concrete in the freeze–thaw environment. *Construction and Building Materials*, 321, 126371.
Zhang, C., Panda, G. P., Yan, Q., Zhang, W., Vipulanandan, C., and Song, G. 2020. Monitoring early-age hydration and setting of portland cement paste by piezoelectric transducers via electromechanical impedance method. *Construction and Building Materials*, 258, 120348.
Zhang, H., Li, J., Kang, F., and Zhang, J. 2022. Monitoring depth and width of cracks in underwater concrete structures using embedded smart aggregates. *Measurement*, 204, 112078.
Zhang, H., Wang, L., Li, J., and Kang, F. 2023. Embedded PZT aggregates for monitoring crack growth and predicting surface crack in reinforced concrete beam. *Construction and Building Materials*, 364, 129979.
Zhang, Y., Miyamori, Y., Mikami, S., and Saito, T. 2019. Vibration‐based structural state identification by a 1‐dimensional convolutional neural network. *Computer-Aided Civil and Infrastructure Engineering*, 34(9), 822-839.
Zhou, X.-Q., Huang, B.-G., Wang, X.-Y., and Xia, Y. 2022. Deep learning-based rapid damage assessment of RC columns under blast loading. *Engineering Structures*, 271, 114949.
Zou, D., Cheng, H., Liu, T., Qin, S., and Yi, T.-H. 2019. Monitoring of concrete structure damage caused by sulfate attack with the use of embedded piezoelectric transducers. *Smart Materials and Structures*, 28(10), 105039.